Received: 13 December 2016 | Revised: 24 May 2017 | Accepted: 15 June 2017

DOI: 10.1002/ett.3216

RESEARCH ARTICLE

WILEY

Divide-and-allocate: An uplink successive bandwidth division NOMA system

Soma Qureshi[1] | Syed Ali Hassan[1] | Dushantha Nalin K. Jayakody[2]

[1]School of Electrical Engineering and Computer Science, National University of Sciences and Technology, Islamabad, Pakistan

[2]Department of Software Engineering, Institute of Cybernetics National Research Tomsk Polytechnic University, Tomsk, Russia

Correspondence
Soma Qureshi, School of Electrical Engineering and Computer Science, National University of Sciences and Technology, Islamabad, Pakistan.
Email: 14mseesqureshi@seecs.edu.pk

Funding information
Ministry of Education and Science of the Russian Federation, Grant/Award Number: 02.G25.31.0190

Abstract

This paper investigates a new spectrum-sharing strategy using non-orthogonal multiple access (NOMA), a technique that is expected to lead toward the fifth generation of wireless networks. The proposed scheme, namely, successive bandwidth division (SBD), NOMA, is a hybrid approach exploiting the characteristics of both the conventional NOMA system and the orthogonal multiple access (OMA) system. Power allocation is being performed in successive bandwidth division NOMA to maximize the sum rate using a divide-and-allocate approach such that all users are allocated with optimal transmission power. Under Rayleigh fading, the probability density function (PDF) of the received signal-to-interference-plus-noise ratio (SINR) is derived, and closed-form expressions for the outage probability are presented when channel state information (CSI) is available at the base station. The performance evaluation is carried out in terms of receiver complexity, average sum rate, and outage probability. Simulations results are provided to access and compare the performance of the proposed scheme with other contemporary approaches.

1 | INTRODUCTION

Recently, many research studies have been focusing on designing future mobile networks, which are capable of supporting the overwhelming demand for data traffic in 2020 and beyond. One of the challenges in meeting the future traffic demand is to be able to provide high spectral efficiency, which is possible by the efficient design of multiple access schemes in future cellular networks in addition to other technologies. The demand to design next-generation wireless networks has long been sought. Several metrics and parameters have been considered as performance measures, eg, spectral efficiency, reliability, quality of service (QoS), and efficient utilization of radio resources and energy efficiency (EE). Researchers from both the industry and academia are exploring the domains of a multitude of techniques for future networks, including device-to-device communication, ultradensification, millimeter-wave communication, massive multiple-input multiple-output (MIMO), and novel multiple access schemes under the umbrella of fifth-generation (5G) networks.[1,2]

The design of an appropriate multiple access method is one of the most significant challenges in optimizing the system capacity. The multiple access methods can be sketchily branded into 2 main methods: orthogonal multiple access (OMA) and nonorthogonal multiple access (NOMA).[3] An orthogonal scheme permits a seamless receiver to completely separate unsolicited signals from the desired signal using different basis functions, ie, signals from separate users are orthogonal to one another in orthogonal schemes. Time-division multiple access (TDMA) and orthogonal frequency-division multiple access (OFDMA) are examples of OMA schemes.

On the other hand, NOMA is considered a candidate multiple access scheme for 5G wireless networks because of its ability to share space resource among multiple users in addition to other benefits being offered. By virtue of this property, NOMA provides higher spectral efficiency, reduced latency, massive connectivity, ultrafast speeds, and user fairness[4] as compared

with the traditional multiple access techniques. The key feature of NOMA is in exploring the multiplexing gain in the power domain. The NOMA system superimposes user signals on top of one another at the transmitter and uses successive interference cancellation (SIC) at the receivers, thus accommodating a large number of users via nonorthogonal resource sharing. Contrary to the conventional water-filling power allocation strategy, the NOMA technique allocates more transmit power to the users with poor channel conditions (ie, weak users) and less transmit power to the users with better channel conditions (ie, strong users) to set the power difference between the users, which allows postcoding to suppress or minimize the interference and exploits the gain from NOMA within users. In this case, the weak users can decode their high-powered signals directly by treating other signals as noise. In contrast, those users with better channel conditions (ie, strong users) adopt the SIC technique for signal detection. This way, the low-powered signals are recovered after SIC.[5] It has been demonstrated that by using superposition coding together with SIC, both the system throughput and user fairness are significantly improved in NOMA systems compared with conventional OMA systems.

1.1 | Literature and motivation

The concept of NOMA is not new as it can be linked to many well-known methods used in previous communication systems. Early works on the NOMA system generally consider a transmitter with a single antenna. However, it can also be extended to various systems. Ding et al[6] studied the ergodic sum rate and outage performance of downlink (DL) NOMA with randomly deployed single-antenna nodes. Hojeij et al[7] characterized other works on resource allocation in DL NOMA. Recently, some attempts have been made to combine NOMA with MIMO to achieve high spectral efficiency as the application of MIMO to NOMA provides additional degrees of freedom.[5] However, the scheme proposed by Ding et al[5] does not need channel state information (CSI) at the transmitter; rather, it requires the larger number of receive antennas as compared with the transmitter. Most of the existing work on MIMO NOMA, such as that by Choi[8] and Sun et al,[9] assumed perfect knowledge of CSI at the transmitter, which is difficult to realize in practice. The perfect CSI assumption can consume high bandwidth particularly in massive MIMO scenarios.[10] In the work of Higuchi and Kishiyama,[11] the authors proposed random opportunistic beamforming for the MIMO-NOMA systems, where the base station (BS) transmitter generates multiple beams and superimposes multiple users within each beam. A massive MIMO-NOMA DL transmission protocol has been recently proposed, which does not require the users to feed their channel matrices back to the BS. Some other works include those by Liu et al[12] and Higuchi and Kishiyama.[13] Various algorithmic frameworks for optimizing the design of beamforming in the NOMA transmission system have been considered in the work of Hanif et al.[14] In the work of Choi,[15] an optimization problem was formulated for various MIMO-NOMA scenarios. A signal alignment–based precoding scheme was developed in the work of Ding et al,[16] which requires fewer antennas at the users compared with the scheme proposed earlier by Ding et al.[5] Power allocation between 2 users is carried out for open-loop MIMO DL transmissions (ie, the BS allocates the power to 2 user signals based on statistical CSI). In the work of Qi et al,[17] a zero-forcing (ZF)-based beamforming and user pairing scheme was proposed for the DL multiuser (MU) NOMA system, assuming perfect CSI at the transmitter. More details on MIMO NOMA can be found in the work of Dai et al.[18] Both papers by Liu et al[19] and Di et al[20] have also worked on the DL scenario. The number of candidate users in the above paper is not more than $N_{\max}$, which is fixed to 2 in that proposed paper. Similarly, Liu et al[19] also solved the power allocation problem for a DL scenario as a many-to-many matching game with externalities and geometric programming, which is one of the efficient methods to solve the resource allocation problem, the other being optimization theory and coalition formation games. An uplink (UL) NOMA transmission scheme was proposed in the work of Kim et al.[21] Similarly, in the work of Ding et al,[22] the impact of user pairing was characterized by analyzing the sum rates in 2 NOMA systems. Some other existing works[23–26] on the design of UL NOMA for 5G wireless networks have been proposed. Recent works on UL NOMA are those by Endo et al[27] and Sung and Fu.[28] A UL power back-off policy was proposed to distinguish users in a NOMA cluster with nearly similar signal strengths (given that traditional UL power control is applied). Closed-form analysis was performed for the ergodic sum rate and outage probability of a 2 user NOMA cluster. Furthermore, the problem of user scheduling in UL NOMA was investigated by various researchers in the work of Takeda and Higuchi.[29] However, the performance gain in the aforementioned work[29] is limited due to the use of naive power control schemes such as fixed power allocation (FPA) and fixed transmission power control for multiplexed users. Joint subcarrier allocation and power control in UL NOMA was investigated in the work of Endo et al[30] with perfect SIC at the BS, which is proved to be NP-hard and solved by a near-optimal solution based on Lagrangian duality and dynamic programming. A game-theoretic algorithm for UL power control was designed in the work of Sung and Fu[31] considering a 2-cell NOMA system, where intercell interference is assumed to be Gaussian distributed. However, most of the previous works on multicarrier (MC) NOMA considers only 2 user scenarios such as in the works of Sung and Fu[31] and Shin et al.[32] The proposed scheme also offers high computational complexity as compared with our work.

Another work on MC NOMA is that by Fu et al.[33] In conventional MC systems, a given radio frequency band is divided into multiple orthogonal subcarriers, and each subcarrier is allocated to, at most, 1 user to avoid MU interference. The spectral efficiency of such systems can be improved significantly by performing joint user scheduling and power allocation. In fact, spectral efficiency can be further improved by applying NOMA in MC systems by exploiting the degrees of freedom offered by MU diversity and the power domain simultaneously. In the work of Saito et al,[4] the authors demonstrated that MC-NOMA systems employing a suboptimal power allocation scheme achieve system throughput gains over conventional MC-OMA systems. Lei et al[34] proposed a suboptimal joint power and subcarrier allocation algorithm for MC-NOMA systems. However, the resource allocation schemes proposed in the aforementioned works[4,34] are strictly suboptimal. Some other significant works include the combination of NOMA with cooperative communications and millimeter wave, which has been characterized in the works of Ding et al[35] and Naqvi and Hassan.[36] The system-level performance of an OFDMA-based NOMA system with fractional transmit power allocation (FTPA) and equal transmit power allocation (ETPA) was considered in the work of Saito et al.[37] Some other work on power allocation has been discussed in the works of Al-Abbasi and So[38] and Parida and Das.[39] Otao et al[40] presented different power allocation schemes for NOMA considering FTPA, full search power allocation, and FPA. Full search power allocation performs well, but it has high computational complexity; FPA has worse performance but least complexity; whereas FTPA is a balance between the two but does not distribute power among the multiplexed users in an optimum way to maximize the sum rate. Similarly, in these existing works, the maximum achievable improvement in the spectral efficiency of optimal MC-NOMA systems compared with MC-OMA systems is also still unknown. Therefore, for a UL OFDMA-based NOMA system, we have proposed a hybrid multiple access scheme. Compared with these existing works, the motivations of this paper are as follows.

In conventional OMA schemes, multiple users are allocated with radio resources that are orthogonal in the time, frequency, or code domain. Ideally, no interference arises due to orthogonal resource allocation; hence, simple single-user detection can be used to separate different user signals. On the other hand, NOMA allows controllable interference by nonorthogonal resource allocation at the expense of enhanced receiver complexity. In NOMA, all the users can use resources simultaneously, which leads to interuser interference. Hence, more complicated MU detection (MUD) techniques are required to retrieve the user signals at the receiver. The optimal approach for UL NOMA is to allow all the users to share each resource element, and the users' power allocated through iterative water-filling.[41] However, in the optimal (unconstrained) NOMA scheme, there is no control over the number of users that share each subcarrier, which makes the MUD at the receiver infeasible. This problem can be mitigated by imposing an upper limit on the number of users per resource to reduce the receiver complexity. In order to further reduce the interference, we have also divided the available bandwidth into identical orthogonal groups. The proposed scheme not only reduces the number of MUD but also offers reduced complexity and interference. It also eliminates the need for complex receiver designing, which reduces the cost and provides enhanced QoS. Hence, situations where user priority is reduced cost and enhanced QoS, successive bandwidth division (SBD) NOMA schemes should be preferred over conventional UL NOMA, which provide a better rate and a fairly reliable transmission scheme. Therefore, to manage the interset interference efficiently, for the UL of an OFDMA-based NOMA system, we propose a suboptimal algorithm known as SBD-NOMA. As the proposed scheme involves a hybrid multiple access scheme as SBD-NOMA, consisting of both orthogonal and nonorthogonal transmissions, it therefore inherits the advantages of both techniques. In the proposed scheme, the total number of users is orthogonally divided into different subbands on the basis of their CSI with limited number of users in each subband. Depending upon the number of users in each subband, the total bandwidth is divided into orthogonal groups. "Hence, the SBD scheme divides the available bandwidth W, of K users, into K/P identical orthogonal subbands, each having a bandwidth of W_{sb}, where P is the number of users in each subband. Hence, the successive addition of users in the system divides the bandwidth successively into orthogonal bands." Because of the orthogonality among the group of users, no joint processing is required at the receiver side to retrieve the user signals. As the proposed scheme captured the aforementioned properties, we name it the SBD-NOMA scheme. To illustrate the concept further, please see Figure 1. In this Figure, the users are occupying the whole available bandwidth in the case of a NOMA system. It accommodates all users in the same frequency band. This is not the case with OMA. In OMA, all the users have separate identical orthogonal subbands. The bandwidth available to each user reduces by a factor of $1/K$. There is a single user in each subband, and the resource blocks allocated are completely orthogonal. For SBD-NOMA, the users are divided into identical orthogonal subbands. However, there does not exist a single user for a single subband. The number of users in each subband is P. The total number of subbands is $K = P$. For $P = 2$, SBD-NOMA specializes to NOMA_2; for $P = 4$, SBD-NOMA specializes to NOMA_4. Similarly, for $P = 8$, SBD-NOMA specializes to NOMA_8. In order to further reduce the interset interference, the users within the same subband are paired. The users paired within the same subband are members of 2 distinct sets, namely, strong set and weak set. The sets are classified on the basis of the channel conditions. The members of the weak set should be chosen in a way that they offer very little or no interference to the other users within the same subband. As the proposed system is formed by combining OMA and NOMA techniques, it inherits the advantages of both techniques.

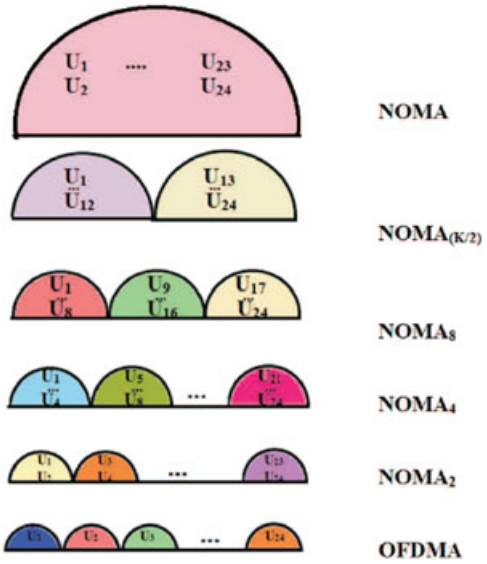

FIGURE 1 Orthogonal frequency-division multiple access (OFDMA) vs nonorthogonal multiple access (NOMA) and the proposed successive bandwidth division scheme; $K = 24$ for this particular example

However, grouping cannot exploit the full potential of NOMA, and for that, we perform optimal power allocations. In this paper, we mainly focus on the power allocation for MIMO NOMA when CSI is available at the BS. The main contributions of this paper are as follows.

- We first consider an OFDMA-based MIMO-NOMA UL scenario, known as SBD-NOMA, with a fixed set of power allocation coefficients. There are many differences between a UL and a DL NOMA system in terms of implementational complexity, intracell/intracluster interference, SIC at the receiver, etc, which can be found in the work of Tabassum et al.[42] The performance of this proposed SBD-NOMA system is characterized with conventional OMA by using the criteria of sum capacity and outage probability.
- An approach to perform the optimal power allocation coefficients for SBD-NOMA with a transmission power constraint is proposed. This is because the choice of the power allocation coefficients is key to achieving a favorable throughput-fairness trade-off in NOMA systems. Analytical results, such as exact expressions of power allocation coefficients, are derived for a 2 user scenario under a total power constraint.
- Under Rayleigh fading, the probability density function (PDF) of the received signal-to-interference-plus-noise ratio (SINR) is approximated by a gamma distribution, and closed-form expressions for the outage probability are presented for SBD-NOMA with no intraset interference.

1.2 | Organization

This paper is organized as follows. Section 2 presents the system model of the UL SBD-NOMA scheme with multiple antennas along with the algorithm for strong and weak set formation and subchannel allocation. Section 3 formulates the sum rate maximization problem and discusses the optimal solutions for a 2 user scenario. Closed-form expressions of outage probability are derived in Section 4. Simulation results and discussion are provided in Section 5. This paper is concluded with some remarks in Section 6.

1.3 | Notation

Matrices and vectors are denoted by uppercase and lowercase boldface letters, respectively. Superscripts $(.)^{\intercal}$, $(.)^{-1}$, and $(.)^{*}$ denote the transpose, inverse, and complex conjugate, respectively. For a matrix $\mathbf{H}$, $h_{i,m}$ represents the (i, m)th element of $\mathbf{H}$. The $\mathbb{CN}$ (0,1) represents the distribution of circularly symmetric complex Gaussian random vector with zero mean and unit variance.

2 | SYSTEM MODEL

This paper considers a UL MU-MIMO scenario, where a BS, equipped with N antennas, communicates with K single-antenna users, where $K \geq 2N$. The transmission occurs in the presence of additive white Gaussian noise (AWGN) over Rayleigh flat fading channels with path loss. In schemes other than NOMA, like a conventional UL system with N BS antennas, only N users can be supported at any instance without interference. The novelty of the proposed UL scheme is that the BS can support $2N$ randomly deployed users at any given instance by superposition coding. In this paper, the term "set" refers to N randomly deployed users chosen on the basis of the channel gains. The sets are classified as *strong* if the corresponding channel gains are large and *weak* if the corresponding channel gains are small. The sets are determined by sorting the channel gains in descending order and then dividing the channel gains into 2 halves. The sets thus formed are assumed to be mutually exclusive.

The OMA scheme divides the entire available spectrum into K subbands, and all K users can be supported simultaneously without any interference. However, the bandwidth available to each user reduces by a factor of $1/K$ for the sake of ensuring orthogonality. For the proposed NOMA system, the users are squashed in the same frequency band. As NOMA accommodates all users in the same frequency band, the interference among users is quite high. Therefore, to efficiently manage the intraset interference in NOMA-assisted networks, the proposed technique works as follows.

2.1 | Proposed SBD scheme

The SBD scheme divides the available bandwidth W, of K users, into K/P identical orthogonal subbands, each having a bandwidth of W_{sb}. Here, P denotes the maximum number of users that can share a subband, where $\{P \in \mathbb{N} \mid 1 \leq P \leq K\}$, and $\mathbb{N}$ is a set of natural numbers. The number P leads to the formation of subbands with different bandwidths, depending on its value. The superposition of relatively small number of users in each subband reduces the receiver complexity, and simple user detection techniques can be applied at the receiver side. The P users paired within the same subband are chosen from 2 mutually exclusive sets A and B whose channel coefficients are pairwise orthogonal.

To get some more insight, consider Figure 1, where the concept of SBD-NOMA is demonstrated. Let the total number of users $K = 24$. For subsequent discussion in this paper, we define a set ϕ, which is the set of the factors of K. For $K = 24$, $\phi = \{1, 2, 3, 4, 6, 8, 12, 24\}$. Since the users paired within each subband are assumed to be equal, hence all even elements from ϕ are chosen. Note that when $P = 1$, the conventional OMA scheme works for each subband, and when $P = K$, the SBD scheme specializes to conventional NOMA. For $P = 2$, the access scheme is denoted as NOMA_2, where the number of users in each subband is 2 while the total subbands are 12. The number P further divides the strong and weak sets A and B into K/P smaller sets such that $\sum_{m=1}^{K/P} A_m \cup B_m = \xi$, where ξ is a set of all K users and with m being the subband index. Each A_m and B_m from sets A and B has a cardinality of 1 for $P = 2$, whereas there is a single interferer in this case. Similarly, for $P = 4$, SBD-NOMA has 4 users in each subband. Each A_m and B_m from sets A and B has a cardinality of 2, whereas the number of interferers is 3 in this case. $P = K$ specializes to the case of conventional UL NOMA, with only 1 subband and $(K - 1)$ interferers. In other words, we define NOMA_P to be the access scheme where K/P subbands are formed with P users in each subband, and a conventional NOMA scheme works in each of the subbands.

The number P will affect the number of subbands, interferers, dimensions of channel and detection matrices, dimensions of received signal, and the number of users in each subband. However, the total number of users remains the same. As only P users can transmit their signals at any given instance, hence the received signal is the superposition of the signals from P users. The remaining users are orthogonal. Therefore, in the proposed UL SBD scheme, the decoding complexity is $O(|\chi|^P)$, whereas that of conventional NOMA with K users is $O(|\chi|^K)$, where χ denotes the constellation alphabet. This is the worst-case complexity. For higher-order modulation schemes, we have other more efficient and reduced complexity algorithms like sphere decoding. There is also an option to use parallel processing for higher-order modulation decoding. However, dividing the entire bandwidth into subbands cannot exploit the full potential of NOMA, where all users can occupy the entire bandwidth. Therefore, to cope with this, we perform optimal power allocation in SBD-NOMA, which provides an achievable rate much better than the one achieved without power allocation.

2.2 | Received signal model for the proposed UL SBD-NOMA

Let us denote the channel matrices of the strong and weak sets as $\mathbf{H}_1$ and $\mathbf{H}_2$, respectively, written as

$$\mathbf{H}_1 = \left[\mathbf{h}_{1,1}\ \mathbf{h}_{1,2}\ \ldots\ \mathbf{h}_{1,P/2}\right], \tag{1}$$

$$\mathbf{H}_2 = \left[\mathbf{h}_{2,1}\ \mathbf{h}_{2,2}\ \ldots\ \mathbf{h}_{2,P/2}\right], \tag{2}$$

where $\mathbf{h}_{1,j}$ and $\mathbf{h}_{2,n}$ denote the $(N \times 1)$ UL channel vectors of the j^{th} strong and the n^{th} weak user, respectively, and are drawn from the complex Gaussian distribution with zero mean and unit variance. The channel vectors are Rayleigh flat faded with path loss. Thus, in the given scenario, the superimposed signal received by the entire group of P users, multiplexed on the mth subband, where $1 \leq m \leq K/P$, is given by

$$\mathbf{y} = (\mathbf{H}_1\mathbf{s}_1 + \mathbf{H}_2\mathbf{s}_2) + \mathbf{n}, \tag{3}$$

where $\mathbf{y}$ is an $(N\times 1)$ UL received signal vectors, and $\mathbf{s}_1 = \left[\sqrt{\alpha_{1,1}}x_{1,1} \ldots \sqrt{\alpha_{1,P/2}}x_{1,P/2}\right]^{\mathsf{T}}$ and $\mathbf{s}_2 = \left[\sqrt{\alpha_{2,1}}x_{2,1} \ldots \sqrt{\alpha_{2,P/2}}x_{2,P/2}\right]^{\mathsf{T}}$ are $(P/2 \times 1)$ signal vectors of strong and weak sets, respectively. Here, $(\cdot)^{\mathsf{T}}$ denotes the transpose, $\alpha_{i,j}$ represents the NOMA power allocation coefficient of strong and weak users, and $x_{i,j}$ represents the symbol transmitted by the j^{th} user to the BS with N antennas and i being a member of the strong or the weak set. The $\mathbf{n}$ is an $(N\times 1)$ AWGN vector, where each value is a normal random variable (RV) with zero mean and unit variance. The total number of signals received by the BS is K/P, and it depends on the number of users within a particular subband.

The received signal of an n^{th} strong user, chosen from set J, where $J = \{1, 2, \ldots, P/2\}$, and $n \in J$ is the superimposed signal given by

$$\mathbf{y}_n = \mathbf{h}_{1,n}\sqrt{\alpha_{1,n}}x_{1,n} + \sum_{j=1}^{P/2}\mathbf{h}_{2,j}\sqrt{\alpha_{2,j}}x_{2,j} + \mathbf{n}, \tag{4}$$

where $\mathbf{h}_{1,n}$ and $\mathbf{h}_{2,n}$ are the $(N\times 1)$ UL channel vectors of the n^{th} user from both strong and weak sets to the BS having N antennas, and $\mathbf{n}$ is the $(N \times 1)$ AWGN vector.

Since the BS receives superimposed signals, an SIC scheme is required at the receiver side for decoding, the signals of the strong set are decoded first, with interference from the weak set, while the users in the weak set are free from interset interference. The remaining users are orthogonal and offer no interset interference.

As this paper assumes perfect CSI, a ZF postcoded or detection matrix is used to decode the signals of strong and weak sets. The corresponding postcoding matrix $\mathbf{Z}_i$ is given by

$$\mathbf{Z}_i = \left[\mathbf{z}_{i,1}^{\mathsf{T}}\ \mathbf{z}_{i,2}^{\mathsf{T}}\ \cdots\ \mathbf{z}_{i,P/2}^{\mathsf{T}}\right]^{\mathsf{T}} = (\mathbf{H}_i)^*((\mathbf{H}_i)(\mathbf{H}_i)^*)^{-1}. \tag{5}$$

In the above equation, $\mathbf{Z}_1$ is the $(P/2\times N)$ postcoded matrix of users in the strong set, and $\mathbf{z}_{i,j}$ is the $(1\times N)$ vector corresponding to the ZF UL channel vector of the j^{th} user, respectively. The application of the postcoded ZF matrix at the receiver forms N decoupled data substreams, which makes the system MIMO NOMA rather than multiple-input single-output (MISO) NOMA.

2.3 | Received SINR

In order to determine the SINR of strong and weak users, respectively, we apply the postcoded matrix $\mathbf{Z}_1$ to decode the users of the strong set, where the received signal vector $\mathbf{r}^{(1)} = \left[r_{1,1}, r_{1,2}, \ldots, r_{1,P/2}\right]$ becomes

$$\mathbf{r}^{(1)} = \mathbf{Z}_1\mathbf{y} = \mathbf{Z}_1\mathbf{H}_1\mathbf{s}_1 + \mathbf{Z}_1\mathbf{H}_2\mathbf{s}_2 + \mathbf{Z}_1\mathbf{n}, \tag{6}$$

where $\mathbf{r}^{(1)}$ is a $(P/2 \times 1)$ received signal vector. From Equation 6, the signal of the n^{th} user in the strong set, chosen from set J, where $n \in J$ is as follows:

$$r_{1,n}^{(1)} = \mathbf{z}_{1,n}\mathbf{h}_{1,n}\sqrt{\alpha_{1,n}}x_{1,n} + \sum_{j=1}^{P/2}\mathbf{z}_{1,n}\mathbf{h}_{2,j}\sqrt{\alpha_{2,j}}x_{2,j} + \mathbf{z}_{1,n}\mathbf{n}. \tag{7}$$

The corresponding SINR of an n^{th} strong user is given by

$$\text{SINR}_{1,n} = \frac{|\mathbf{h}_{1,n}\cdot\mathbf{z}_{1,n}|^2\alpha_{1,n}}{\sum_{j=1}^{P/2}|\mathbf{h}_{2,j}\cdot\mathbf{z}_{1,n}|^2\alpha_{2,j} + \sigma_n^2}, \tag{8}$$

where $|.|$ denotes the norm operator, and $(\mathbf{a}\cdot\mathbf{b})$ represents the point-to-point multiplication between any 2 vectors $\mathbf{a}$ and $\mathbf{b}$. The $|\mathbf{h}_{1,n}\cdot\mathbf{z}_{1,n}|^2\alpha_{1,n}$ represents the desired signal of the n^{th} strong user from set J, whereas the signal $\sum_{j=1}^{P/2}|\mathbf{h}_{2,j}\cdot\mathbf{z}_{1,n}|^2\alpha_{2,j}$ represents the interset interference from weak users. The users are experiencing the intraset interference. The strong and weak users will encounter interference from other strong and weak users, respectively. However, by choosing the transmit antennas more than or equal to receive antennas, the postcoded ZF matrix formed at the receiver is perfectly square, which automatically eliminates the interference from other strong and weak users within the same set. In this case, each channel vector and the ZF postcoding vector satisfy the following condition:

$$\mathbf{z}_{1,j}\cdot\mathbf{h}_{1,n} = 0; \quad \forall j \neq n, \quad j \in \{1, 2, \ldots, P/2\}. \tag{9}$$

However, when the BS is equipped with less than N antennas, then the resultant matrix becomes rectangular. Thus, the strong and weak users also encounter the interference from other strong and weak users, respectively. Consequently, the strong set is affected by a total interference of I, which can be expanded as

$$I = \sum_{j=1, j\neq n}^{P/2} |\mathbf{h}_{1,j} \cdot \mathbf{z}_{1,n}|^2 \alpha_{1,j} + \sum_{j=1}^{P/2} |\mathbf{h}_{2,j} \cdot \mathbf{z}_{1,n}|^2 \alpha_{2,j}, \tag{10}$$

and the corresponding SINR becomes

$$\mathrm{SINR}_{1,n} = \frac{|\mathbf{h}_{1,n} \cdot \mathbf{z}_{1,n}|^2 \alpha_{1,n}}{I + \sigma_n^2}, \tag{11}$$

where $\sum_{j=1,j\neq n}^{P/2} |\mathbf{h}_{1,j} \cdot \mathbf{z}_{1,n}|^2 \alpha_{1,j}$ represents the intraset interference from the other strong users, respectively.

For decoding of weak user signal, SIC is carried out so there will be no interference in this case. Hence, after applying the ZF matrix, the signals of the weak set become

$$\mathbf{r}^{(2)} = \mathbf{Z}_2 \mathbf{H}_2 \mathbf{s}_2 + \mathbf{Z}_2 \mathbf{n}. \tag{12}$$

The received signal and corresponding SINR of the n^{th} weak user chosen from set J becomes

$$r_{2,n}^{(2)} = \mathbf{z}_{2,n} \mathbf{h}_{2,n} \sqrt{\alpha_{2,n}} x_{2,n} + \mathbf{z}_{2,n} \mathbf{n}, \tag{13}$$

$$\mathrm{SINR}_{2,n} = \frac{|\mathbf{h}_{2,n} \cdot \mathbf{z}_{2,n}|^2 \alpha_{2,n}}{\sigma_n^2}. \tag{14}$$

In the case of intraset interference, we have

$$\mathrm{SINR}_{2,n} = \frac{|\mathbf{h}_{2,n} \cdot \mathbf{z}_{2,n}|^2 \alpha_{2,n}}{\sum_{j=1,j\neq n}^{P/2} |\mathbf{h}_{2,j} \cdot \mathbf{z}_{2,n}|^2 \alpha_{2,j} + \sigma_n^2}. \tag{15}$$

The rate of the strong and weak users in SBD-NOMA across any subband is given by

$$R_{im} = W_{\mathrm{sb}} \sum_{j=1}^{P/2} \log_2 \left(1 + \mathrm{SINR}_{i,j}\right); \quad i \in \{1, 2\}, \tag{16}$$

wherein W_{sb} is the subband bandwidth.

The summation of P users over all subbands m is K, where $K \in \xi$ is the total number of users, and it belongs to set ξ. In other words, we can say that $n \in J \wedge J \in \xi$. The total sum rate of the system is given by

$$R_{\mathrm{sum}} = \sum_{i=1}^{2} \sum_{m=1}^{K/P} R_{im}. \tag{17}$$

Finally, the sum capacities of conventional OMA are written as

$$R_{i,\mathrm{OMA}} = W/K \sum_{k=1}^{K} \log_2 \left(1 + \frac{|\mathbf{z}_{i,k} \cdot \mathbf{h}_{i,k}|^2 \alpha_{i,k}}{\sigma_k^2}\right). \tag{18}$$

From Equation 17, it can be seen that the user power has a direct effect not only on the individual user data rate but also on the SINR of other users, which shows the importance of power allocation in an SBD-NOMA system.

2.4 | Channel allocation algorithm

In the proposed UL SBD-NOMA scheme, both conventional OMA and NOMA techniques are implemented simultaneously; therefore, the question of user selection in a set is important. This is because user pairing has the potential of reducing the complexity at the receiver side. The user pairing strategy affects the overall throughput of the proposed scheme. Careful user pairing not only improves the sum rate but also has the potential to improve the individual user rates. Grouping is done on the basis of the channel gains between the users. The pairwise orthogonal users are grouped together in the same subband to get full benefit of the NOMA within each subband. The proposed user pairing algorithm reduces the number of MUD required at the

TABLE 1 Set formation and subchannel allocation algorithm

Initialization
1 A set ξ of K users, where $K = \{1, \dots, k\}$
2 Subchannel allocation matrix, $\mathbf{M} = 0_{(K \times N)}$
3 Number of antennas, N
Channel allocation
Step 1) BS creates M from reported CSI values, $\mathbf{M} = \{\mathbf{h}_1, \mathbf{h}_2, \dots, \mathbf{h_k}\}$.
Step 2) The channel gains are sorted in descending order, forming a set $\mathbf{M}_{\text{ord}}$: $\mathbf{M}_{\text{ord}} = \{\lvert\mathbf{h}_1\rvert^2, \lvert\mathbf{h}_2\rvert^2, \dots, \lvert\mathbf{h_k}\rvert^2\}$ where $\lvert\mathbf{h_K}\rvert^2 > \lvert\mathbf{h_{K+1}}\rvert^2$ and $K \in \{1, 2, \dots, k\}$.
Step 3) The parent set is split into 2 halves: $\mathbf{H}_1 = \{\lvert\mathbf{h}_1\rvert, \lvert\mathbf{h}_2\rvert, \dots, \lvert\mathbf{h}_{\lfloor \mathbf{K}/2 \rfloor}\rvert\}$, $\mathbf{H}_2 = \{\lvert\mathbf{h}_{\lfloor \mathbf{K}/2 \rfloor+1}\rvert, \lvert\mathbf{h}_{\lfloor \mathbf{K}/2 \rfloor+2}\rvert, \dots, \lvert\mathbf{h_K}\rvert\}$, where $\lfloor . \rfloor$ denotes the floor function. The first half is taken to bea strong set A, whereas the other is a weak set B. In $\mathbf{H}_1$, the N users having the higher channel gains are paired. Similarly, in $\mathbf{H}_2$, the N users having lower channel gains are paired:
$\mathbf{H}_1 = \{\lvert\mathbf{h}_{1,1}\rvert, \lvert\mathbf{h}_{1,2}\rvert, \dots, \lvert\mathbf{h}_{1,\lfloor \mathbf{K}/2 \rfloor}\rvert\}$,
$\mathbf{H}_2 = \{\lvert\mathbf{h}_{2,\lfloor \mathbf{K}/2 \rfloor+1}\rvert, \lvert\mathbf{h}_{2,\lfloor \mathbf{K}/2 \rfloor+2}\rvert, \dots, \lvert\mathbf{h}_{2,\mathbf{K}}\rvert\}$.
Step 4) Pair orthogonal users head to tail.
Step 5) For SBD-NOMA, each Rayleigh fading channel matrix divides itself into smaller matrices with dimension $(N \times P/2)$, where P denotes the access scheme. The smaller channel matrices and the corresponding user indexes of strong and weak sets satisfy the condition $\sum_{m=1}^{K/P} A_m \cup Bm = \xi$.
Go to 5).
End When all the N users from the 2 sets are paired in subbands.
Note: The subscript i representing the index of being a strong and weak set has been introduced in the definition of channel gains for notational consistency and clarification.

receiver side. It also offers reduced interference by removing intercluster and interset interference. It also eliminates the need for complex receiver designing, which reduces the cost and provides enhanced QoS. The detailed algorithm for choosing the members of the strong and weak sets is presented in Table 1. The algorithm aims to minimize the interference offered by the weak users to the strong users.

3 | POWER ALLOCATION

In the previous section, constant power allocation coefficients are considered. By constant power allocation coefficients, we mean that both users (ie, strong and weak users) have equal power. In this case, we have not followed the conventional power allocation policy which states that it allocates more transmit power to the users with poor channel conditions (ie, weak users) and less transmit power to the users with better channel conditions (ie, strong users) to set the power difference between the users, which allows postcoding to suppress or minimize the interference and exploits the gain from NOMA within users. However, in this section, more sophisticated choices of power allocation are considered. In this section, we worked on giving unequal power allocation coefficients to NOMA on the basis of instantaneous channel conditions. This helps in further improving the performance of the MIMO-NOMA system. However, dividing the users into orthogonal groups cannot exploit the full potential of NOMA with the exception that the complexity at the receiver side is reduced. This leads to the formation of the SBD-NOMA system with optimal power allocation. The main purpose is to maximize the sum rate across all subbands by allocating optimal power and provide some degree of fairness to each user. The corresponding resource allocation problem considers the number of users in each subband, the choice of user pairing, and the power allocated to each subband. The framed optimization problem maximizes the sum rate and, at the same time, ensures fairness in the system. For the sake of simplicity, we are assuming 2 users in each subband while the total number of users is K. Instead of allocating power values to each subband through iterative water-filling, the power allocated across each subband is assumed to be equally allocated, which would reduce the signaling overhead and complexity of the proposed numerical solutions. However, in general, the sum rate is not convex in nature for more than 2 transmitting sources; hence, the solution is proposed here for NOMA.[2]*

Lemma 1. *The achievable sum rate of the system is concave in nature for more than 2 transmitting sources.*

*The numerical solution for other schemes is not proposed here due to a duality gap in the transformation from a nonconvex into a convex function.

Proof. See Appendix A. □

Mathematically, the problem is formulated as follows:

$$\begin{aligned} \underset{\alpha_{i,j}}{\text{maximize}} \quad & R_{im} \\ \text{subject to} \quad & \alpha_{1,j} + \alpha_{2,j} \leq P_T, \forall j \\ & \alpha_{i,j} \geq 0, \forall i, \forall j \\ & R_{im,j} \geq r_{\min}, \text{where} \quad j \in J, \end{aligned} \tag{19}$$

where Equation 19 represents the constraints of the framed optimization problem, P_T is the total power allocated to users within a particular subband, R_{im} represents the data rate across each subband, $R_{im,j}$ represents the individual data rate of the j^{th} user, and $r_{\min}$ represents the minimum target rate to maintain fairness among the users. The users are already paired and are chosen from 2 distinct sets to reduce the interset interference. Taking into account the objective function described above and solving the optimization problem through Lagrange multipliers lead to the following formulation of the objective function denoted by F:

$$F = R_{im} + \sum_{j=1}^{P/2} \lambda_j (P_T - \alpha_{1,j} - \alpha_{2,j}) + \sum_{j=1}^{P/2} \kappa_j (R_{1m,j} - r_{\min}) + \sum_{j=1}^{P/2} \tau_j (R_{2m,j} - r_{\min}), \tag{20}$$

where λ_j, κ_j, and τ_j represent the Lagrange multipliers. Using the standard procedure, by differentiating F with respect to all $\alpha_{1,j}$ and $\alpha_{2,j}$ and by setting them equal to zero, we obtain a set of $5|J|$ nonlinear equations having $5|J|$ unknowns, where $|J|$ denotes the cardinality of set J. For the sake of simplicity, the derivatives here are taken only for $\alpha_{1,j}$, $\alpha_{2,j}$, τ_j, λ_j, and κ_j. A similar procedure can be used for other variables as well. The entire procedure is repeated over all subbands to maximize the overall sum rate. We obtain

$$\partial F/\partial \alpha_{1,j} = \frac{W_{\text{sb}} \|\mathbf{z}_{1,j} \cdot \mathbf{h}_{1,j}\|^2}{\|\mathbf{z}_{1,j} \cdot \mathbf{h}_{2,j}\|^2 \alpha_{2,j} + \sigma_j^2 + \|\mathbf{z}_{1,j} \cdot \mathbf{h}_{1,j}\|^2 \alpha_{1,j}} - \lambda_j - \kappa_j \frac{W_{\text{sb}} \|\mathbf{z}_{1,j} \cdot \mathbf{h}_{1,j}\|^2}{\|\mathbf{z}_{1,j} \cdot \mathbf{h}_{2,j}\|^2 \alpha_{2,j} + \sigma_j^2 + \|\mathbf{z}_{1,j} \cdot \mathbf{h}_{1,j}\|^2 \alpha_{1,j}}, \tag{21}$$

$$\begin{aligned} \partial F/\partial \alpha_{2,j} = & \frac{\|\mathbf{z}_{2,j} \cdot \mathbf{h}_{2,j}\|^2}{\|\mathbf{z}_{2,j} \cdot \mathbf{h}_{2,j}\|^2 \alpha_{2,j} + \sigma_j^2} - \lambda_j - \frac{W_{\text{sb}} \|\mathbf{z}_{1,j} \cdot \mathbf{h}_{1,j}\|^2 \|\mathbf{z}_{1,j} \cdot \mathbf{h}_{2,j}\|^2 \alpha_{1,j}}{\|\mathbf{z}_{1,j} \cdot \mathbf{h}_{2,j}\|^2 \alpha_{2,j} + \sigma_j 2 + \|\mathbf{z}_{1,j} \cdot \mathbf{h}_{1,j}\|^2 \alpha_{1,j} \varphi} \\ & + \kappa_j \frac{W_{\text{sb}} \|\mathbf{z}_{1,j} \cdot \mathbf{h}_{1,j}\|^2 \|\mathbf{z}_{1,j} \cdot \mathbf{h}_{2,j}\|^2 \alpha_{1,j}}{\|\mathbf{z}_{1,j} \cdot \mathbf{h}_{2,j}\|^2 \alpha_{2,j} + \sigma_j^2 + \|\mathbf{z}_{1,j} \cdot \mathbf{h}_{1,j}\|^2 \alpha_{1,j} \varphi} + \tau_j \frac{W_{\text{sb}} \|\mathbf{z}_{2,j} \cdot \mathbf{h}_{2,j}\|^2}{\sigma_j^2}, \end{aligned} \tag{22}$$

where $\varphi = \|\mathbf{z}_{1,j} \cdot \mathbf{h}_{2,j}\|^2 \alpha_{2,j} + \sigma_j^2$. Furthermore, we have

$$\partial F/\partial \lambda_j = P_T - \alpha_{1,j} - \alpha_{2,j}, \tag{23}$$

$$\partial F/\partial \kappa_j = W_{\text{sb}} \log_2 \left(1 + \frac{\|\mathbf{z}_{1,j} \cdot \mathbf{h}_{1,j}\|^2 \alpha_{1,j}}{\|\mathbf{z}_{1,j} \cdot \mathbf{h}_{2,j}\|^2 \alpha_{2,j} + \sigma_j^2} \right) - r_{\min}, \tag{24}$$

$$\partial F/\partial \tau_j = W_{\text{sb}} \log_2 \left(1 + \frac{\|\mathbf{z}_{2,j} \cdot \mathbf{h}_{2,j}\|^2 \alpha_{2,j}}{\sigma_j^2} \right) - r_{\min}, \tag{25}$$

$$\alpha_{1,j} \cdot \partial F/\partial \alpha_{1,j} = 0, \tag{26}$$

$$\alpha_{2,j} \cdot \partial F/\partial \alpha_{2,j} = 0, \tag{27}$$

$$\lambda_j \cdot \partial F/\partial \lambda_j = 0, \tag{28}$$

$$\kappa_j \cdot \partial F/\partial \kappa_j = 0, \tag{29}$$

$$\tau_j \cdot \partial F/\partial \tau_j = 0, \tag{30}$$

where $\alpha_{1,j}, \alpha_{2,j}, \lambda_j, \kappa_j, \tau_j \geq 0$. Solving Equation 21 for the Lagrange variable λ_j and substituting it in Equation 22, the value of $\alpha_{2,j}$ from Equation 23 gives the value of $\alpha_{1,j}$, which turns out to be

$$\begin{aligned} \alpha_{1,j} = & \frac{2(\varphi_{aj} - \varphi_{cj})\varphi_{bj}(\varphi_{bj}(1 + \tau_j)\left(\sigma_j^2 + \varphi_{cj} P_T\right) + \varphi_{aj}(1 + \kappa_j)(\Psi_1))}{2(\varphi_{bj})^2(\varphi_{aj} - \varphi_{cj})(\varphi_{cj} + \varphi_{aj}\kappa_j - \varphi_{aj}\tau_j + \varphi_{cj}\tau_j)} \\ & \frac{-2\sqrt{\varphi_{aj}(\varphi_{aj} - \varphi_{cj})\varphi_{bj}^2(1 + \kappa_j)(1 + \tau_j)\left(\sigma_j^2(-\varphi_{cj} + \varphi_{bj}) + \varphi_{aj}(\Psi_1)\right)^2}}{2(\varphi_{bj})^2(\varphi_{aj} - \varphi_{cj})(\varphi_{cj} + \varphi_{aj}\kappa_j - \varphi_{aj}\tau_j + \varphi_{cj}\tau_j)}, \end{aligned} \tag{31}$$

where $\Psi_1 = (\sigma_j^2 + \varphi_{bj} P_T)$, and φ_{aj}, φ_{bj}, and φ_{cj} are given by $\varphi_{aj} = \|\mathbf{z}_{1,j} \cdot \mathbf{h}_{1,j}\|^2$, $\varphi_{bj} = \|\mathbf{z}_{2,j} \cdot \mathbf{h}_{2,j}\|^2$, and $\varphi_{cj} = \|\mathbf{z}_{1,j} \cdot \mathbf{h}_{2,j}\|^2$, respectively. The value of $\alpha_{2,j}$ is derived by substituting the value of $\alpha_{1,j}$ in Equation 23 and is given by

$$\alpha_{2,j} = P_T - \alpha_{1,j}. \tag{32}$$

†

3.1 | Extension to SBD-NOMA with *P* users in each subband

To investigate the scenario of more than 2 users in each subband, multistage power allocation is proposed. In the first stage, the users form 2 distinct sets *A* and *B* on the basis of the algorithm presented in Table 1. After this step, 2 subbands from sets *A* and *B* are formed, each having equal number of users. The power allocated to each subband is equal to half of the total transmission power. In this scenario, the channel gains become the sum of all channel power values in the 2 subbands. The same procedure for SBD-NOMA$_2$ is repeated for power allocation within the 2 subbands. In the second stage, the 2 subbands further divide themselves into smaller subbands, ie, 2 subbands are formed in each subband of the previous stage with the total power per subband as determined in the first stage. In the third stage, these subbands further divide into smaller subbands to allocate power to all users. The procedure is repeated until all users are allocated with optimal transmission power.

The procedure presented above is also applicable to the numbers of users, which are not in power of 2. To illustrate the concept, consider $K = 12$, ie, the total number of users is 12, which is not a power of 2. However, the users can easily be split into 3 subbands having 4 users each. In the second stage, these 4 users further divide themselves into 2 subbands having 2 users in each subband. After that, the power allocation proposed in Section 3 can easily be applicable to the users. For other even number of users, there are many possible combinations. For instance, considering $K = 26$, the users can be split into 2 subbands having 13 users each, or 7 subbands can be formed having 4 users in 6 subbands, and the remaining 2 users can be incorporated in the last one, 13 subbands of 2 users can also be formed. However, in the examples presented above, the number of strong and weak users in the subbands may not be equal and even. There are many possible combinations of grouping in the examples presented above, which is beyond the scope of this paper. The general expression for power allocation in this scenario is given as follows:

$$\sum_{j=1}^{P/2} \alpha_{i,j} = P_T, \forall i. \tag{33}$$

It must be noticed that the constraints in Equations 19 and 33 are the same. Equation 33 gives the same result on expanding the summation for 2 users over *J*, which varies from 1 to $P/2$. However, Equation 19 is written for just 2 users, whereas the constraint has been generalized in Equation 33.

4 | OUTAGE PROBABILITY

The outage probability is an important performance metric as it measures the probability of unsuccessful signal decoding for a given service. The outage probability experienced by any n^{th} user in the weak set can be defined as

$$\begin{aligned} P_o &= 1 - \Pr(\text{SINR}_{2,n} > r_{\min}) \\ &= 1 - \Pr\left(\frac{|\mathbf{h}_{2,n} \cdot \mathbf{z}_{2,n}|^2 \alpha_{2,n}}{\sigma_n^2} > r_{\min}\right). \end{aligned} \tag{34}$$

†In order to present the general idea, we derive the expression of $\alpha_{1,j}$ in terms of Lagrange variables. However, the values of $\alpha_{1,j}$ are numerically solved in MATLAB, and the expressions of Lagrange variables are explicitly not added in this paper.

Building on Equation 34, the outage probability experienced by any n^{th} user in the strong set can be written as

$$\begin{aligned} P_o &= 1 - \Pr(\text{SINR}_{1,n} > r_{\min}) \\ &= 1 - \Pr\left(\frac{|\mathbf{h}_{1,n} \cdot \mathbf{z}_{1,n}|^2 \alpha_{1,n}}{\sum_{j=1}^{P/2} |\mathbf{h}_{2,j} \cdot \mathbf{z}_{1,n}|^2 \alpha_{2,j} + \sigma_n^2} > r_{\min} \right). \end{aligned} \tag{35}$$

In the above expressions, there is no intraset interference. Here, it is assumed that the BS is equipped with N antennas, and hence, the number of interferers from the weak set is also N; therefore, it may be stated that the strong users are only affected by interset interference from the weak users. Furthermore, $\mathbf{Z}_2\mathbf{H}_2 = \mathbf{I}_k$ and $\mathbf{z}_{2,n}\mathbf{h}_{2,j} = \delta_{nj}$, where $\delta_{nj} = 1$ for $n = j$ and 0 otherwise. The same holds true for the strong users as well. We first derive the approximate PDF of the SINR of the users in strong and weak sets, respectively.

4.1 | Approximate PDF of SINR for weak users

To derive the PDF of the SINR of weak users, the SINR given by Equation 14 can be written as

$$\text{SINR}_{2,n} = \frac{\alpha_{2,n}}{\sigma_n^2} \triangleq \frac{\alpha_{2,n}}{\|\mathbf{z}_{2,n}\|^2 \sigma^2} \triangleq \frac{\alpha_{2,n}}{\left[(\mathbf{H}_2^* \mathbf{H}_2)^{-1}\right]_{nn} \sigma^2}. \tag{36}$$

Denoting the SINR defined in Equation 36 with an RV Y, it becomes

$$\text{SINR}_{2,n} = \frac{\alpha_{2,n}}{Y\sigma^2}, \tag{37}$$

where $Y = \left[(\mathbf{H}_2^* \mathbf{H}_2)^{-1}\right]_{nn}$. From Equation 37, it is obvious that we can derive the PDF of SINR provided that the PDF of Y is known. The RV Y in the denominator of Equation 37 is expanded as

$$\left[(\mathbf{H}_2^* \mathbf{H}_2)^{-1}\right]_{nn} = \frac{1}{(\mathbf{h}_{2,n})^* \mathbf{h}_{2,n} - (\mathbf{h}_{2,n})^* \mathbf{H}_{2n} (\mathbf{H}_{2n}^* \mathbf{H}_{2n})^{-1} \mathbf{h}_{2,n} (\mathbf{H}_{2n})^*}, \tag{38}$$

where $\mathbf{H}_{2n}$ is the submatrix obtained after removing the n^{th} column from matrix $\mathbf{H}_2$. Hence, we have

$$\text{SINR}_{2,n} = \frac{\alpha_{2,n} (\mathbf{h}_{2,n})^* \mathbf{h}_{2,n} - (\mathbf{h}_{2,n})^* \mathbf{H}_{2n} (\mathbf{H}_{2n}^* \mathbf{H}_{2n})^{-1} \mathbf{h}_{2,n} (\mathbf{H}_{2n})^*}{\sigma^2}. \tag{39}$$

Generally, for any $N \times K$ Rayleigh fading matrix, the expression in the numerator of Equation 39 follows a gamma distribution with shape parameter $N - K + 1$ and scale parameter 1, ie, $\Gamma(N - K + 1, 1)$. This is because it represents the sum of independent and identically distributed exponential RVs, each having a unit mean, and the PDF is given as

$$f_Y(y) = \frac{y^{(N-K)} \exp(-y)}{\Gamma(N - K + 1)}. \tag{40}$$

However, in the above case, there are N users in each set, and the channel gains are Rayleigh faded with path loss. Therefore, the expression in the numerator of Equation 39 follows a gamma distribution with shape parameter 1 and scale parameter λ_{in}, ie, $\Gamma(1, \lambda_{in})$, where λ_{in} is the mean power experienced by the n^{th} user because of path loss. The $\Gamma(1, \lambda_{in})$, with shape parameter 1, converges to an exponential distribution given by

$$f_Y(y) = \frac{1}{\lambda_{in}} \exp\left(\frac{-y}{\lambda_{in}} \right). \tag{41}$$

Multiplication with power allocation coefficient $\alpha_{2,n}$ and division by the noise variance σ^2, both of which are constants for a particular user, will only change the mean parameter of the RV Y. Hence, the final closed-form expression for the PDF of the SINR of the weak user becomes

$$f_Y(y) = \frac{1}{\tau_{in}} \exp\left(\frac{-y}{\tau_{in}} \right), \tag{42}$$

where τ_{in} is the modified mean. To calculate the outage, first, find the coverage probability by integrating the above expression, and then, we have

$$\Pr(\text{SINR}_{2,n} > r_{\min}) = \int_{r_{\min}}^{\infty} f_Y(y)\, dy. \tag{43}$$

Using Equation 34, we obtain the outage probability of weak users, as follows:

$$\begin{aligned} P_o &= 1 - \Pr(\mathrm{SINR}_{2,n} > r_{\min}), \\ &= 1 - \int_{r_{\min}}^{\infty} f_Y(y)\, dy. \end{aligned} \tag{44}$$

4.2 | Approximate PDF of SINR for strong users

To derive the PDF of SINR of strong users, the SINR given by Equation 8 can be written as

$$\begin{aligned} \mathrm{SINR}_{1,n} &= \frac{\alpha_{1,n}}{\sum_{j=1}^{P/2} |\mathbf{h}_{2,j} \cdot \mathbf{z}_{1,n}|^2 \alpha_{2,j} + |\mathbf{z}_{1,n}|^2 \sigma^2} \\ &\triangleq \frac{\alpha_{2,n}}{\sum_{j=1}^{P/2} |\mathbf{h}_{2,j} \cdot \mathbf{z}_{1,n}\|^2 \alpha_{2,j} + \left[(\mathbf{H}_1^* \mathbf{H}_1)^{-1}\right]_{nn} \sigma^2}. \end{aligned} \tag{45}$$

Denoting the SINR defined in Equation 45 with RV X and T, it becomes

$$\mathrm{SINR}_{1,n} = \frac{\alpha_{1,n}}{X + T\sigma^2}, \tag{46}$$

where $T = \left[(\mathbf{H}_1^* \mathbf{H}_1)^{-1}\right]_{nn}$. To calculate the PDF of the SINR of strong users, we need to calculate the PDF of RV X and T. The PDF of the product of $T\sigma^2$ is already known from above. To derive the density function of interference represented by X, notice that X is a sum of exponential RVs, and its PDF is given by a gamma distribution, ie,

$$X = \sum_{j=1}^{P/2} \|\mathbf{z}_{1,n} \cdot \mathbf{h}_{2,j}\|^2 \alpha_{2,j}, \tag{47}$$

$$f_X(x) = \frac{x^{(v-1)} \exp(-x/\Omega)}{\Gamma(v)\Omega^v}, \tag{48}$$

where $v = \frac{\mathbb{E}[X]^2}{\mathrm{var}[X]}$, and $\Omega = \frac{\mathrm{var}[X]}{\mathbb{E}[X]}$. To derive the analytical expressions for v and Ω, we assume independent interfering signals from weak users, where the power allocation coefficient $\alpha_{2,j}$ is considered as a constant for a particular user. Hence, the mean and variance of X can be written as

$$\mathbb{E}[X] = \sum_{j=1}^{P/2} \alpha_{2,j} \mathbb{E}[W_j], \tag{49}$$

where $W_j = \varphi_{cjn} = \|\mathbf{z}_{1,n} \cdot \mathbf{h}_{2,j}\|^2$, and

$$\mathrm{var}(X) = \sum_{j=1}^{P/2} \alpha_{2,j}^2 \mathrm{var}(W_j). \tag{50}$$

It can be seen that the PDF of W_j is also gamma distributed with a unit scale parameter. The general expression of the PDF for the case of $N \geq K$ can be written as

$$f_W(w) = \frac{K^{N-K+1} \exp(-Kx) w^{N-K}}{\Gamma(N-K)}, \tag{51}$$

$$\mathbb{E}(W_j) = 1, \tag{52}$$

$$\mathrm{var}(W_j) = 1. \tag{53}$$

Therefore, the values of v and Ω are given by

$$v = \frac{\left(\sum_{j=1}^{P/2} \alpha_{2,j}\right)^2}{\sum_{j=1}^{P/2} \alpha_{2,j}^2} \tag{54}$$

and

$$\Omega = \frac{\sum_{j=1}^{P/2} \alpha_{2,j}^2}{\sum_{j=1}^{P/2} \alpha_{2,j}}. \tag{55}$$

Using Equations 54 and 55, the PDF of X can be computed. The PDF of the product $T\sigma^2$ is already known. The addition of 2 independent gamma RVs is also gamma distributed. The numerator of Equation 45 is just a power allocation coefficient $\alpha_{1,n}$, which is considered as a constant; hence, just change the scale parameter of the resultant gamma distribution. Therefore, the final expression for the PDF of SINR can be written as

$$f_U(u) = \frac{u^{(s-1)} \exp(-u/\Omega_w)}{\Gamma(s)\Omega_w^s}, \tag{56}$$

where s and Ω_w are the resultant shape and scale parameters, respectively. To calculate the outage, we have

$$\Pr(\text{SINR}_{1,n} > r_{\min}) = \int_{r_{\min}}^{\infty} \frac{u^{(s-1)} \exp(-u/\Omega_w)}{\Gamma(s)\Omega_w^s} du. \tag{57}$$

Equation 57 can be expanded as

$$\exp\left(\frac{-r_{\min}}{\Omega_w}\right) \sum_{f=o}^{s} \frac{\left(\frac{r_{\min}}{\Omega_w}\right)^f}{f!}. \tag{58}$$

By using the above equation, we can calculate the coverage probability. Hence, by using Equation 35, the outage probability of strong users can be obtained as follows:

$$\begin{aligned} P_o &= 1 - \Pr(\text{SINR}_{1,n} > r_{\min}), \\ &= 1 - \exp\left(\frac{-r_{\min}}{\Omega_w}\right) \sum_{f=o}^{s} \frac{\left(\frac{r_{\min}}{\Omega_w}\right)^f}{f!}. \end{aligned} \tag{59}$$

The outage equations given by Equations 43 and 57 depend upon the number of transmit and receive antennas, the threshold chosen for estimating the outage probability, the number of users in each strong and weak set, and the interference term appearing in the denominator of the SINR. Here, it can be seen that the interference term will greatly affect the overall outage probability of the users.

5 | PERFORMANCE EVALUATION

In this section, the simulation results of the scenarios under discussion are presented. We investigate the performance of the SBD-NOMA system and compare it with the conventional OMA and NOMA techniques, with a fixed set of power allocation coefficients. The cell radius is assumed to be 1000 m, in which all the users are randomly distributed. The value of the radius is chosen only for a fair comparison between different SBD schemes under discussion. The channel coefficients are assumed to be independent and identically distributed Rayleigh flat faded. The transmission power per user is 24 dBm. The noise is assumed to be zero mean circular-symmetric complex Gaussian having a noise density of −174 dBm/Hz. The overall system bandwidth is 4.32 MHz. The path loss is calculated by using the following model:

$$\text{PL}_{\text{dB}} = 30 + 10\beta \log_{10}(d), \tag{60}$$

where d is the distance between the BS and the mobile station, and β is the path loss exponent, which is kept at 4 in this study.

Figure 2 demonstrates the relationship between sum capacity and varying the number of users, K. This Figure compares the sum capacity of OMA, NOMA, and the proposed SBD-NOMA schemes, each having a fixed set of power allocation coefficients. The primary observation is in examining the effect of the number of users on sum capacity in the SBD-NOMA system. The sum capacity improves with the increase in the number of users, but the improvement is not substantial for NOMA_4 and NOMA_8 schemes after the number of users exceeds a certain limit, because of significant interference. However, these schemes offer better coverage probability, and hence, their outage probability is quite low, and they offer less complexity than the

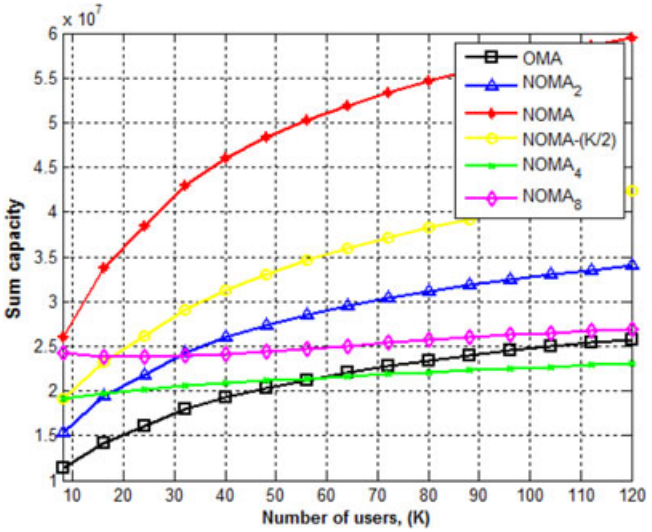

FIGURE 2 Sum capacity comparison between successive bandwidth division nonorthogonal multiple access (NOMA), conventional orthogonal multiple access (OMA), and NOMA techniques

conventional NOMA technique. The inconsistency in performance is due to that SBD-NOMA can reduce the achievable rates as dividing the entire bandwidth into subbands cannot exploit the full potential of NOMA, where all users can occupy the entire bandwidth. As bandwidth is directly proportional to each user's data rate, the effect is visible in the sum capacity analysis. However, dividing the users into orthogonal groups will reduce the intraset interference. The major outcome of sharing is that the sum rate is expected to improve, which can be further enhanced by properly allocating power to weak users. Furthermore, it can be noticed that OMA techniques have a very poor spectrum fairness index among the users. This is because there is exclusivity in resource allocation, ie, a resource block allocated to 1 user cannot be used by any other user. However, the fairness offered by SBD-NOMA is way better than OFDMA with reduced complexity and signaling overhead at the BS. To compare the fairness in SBD-NOMA, NOMA, and OMA techniques, the modified Jain's fairness index (MJFI) can be evaluated, which is given as

$$\text{MJFI} = \frac{\left(\sum_{k=1}^{K/2} \bar{R_{i,k}}\right)^2}{K/2 \sum_{k=1}^{K/2} \bar{R_{i,k}^2}}, i \in \{1,2\}, \bar{R_{i,k}} = \frac{R_{i,k}}{R_{i,k}^{\max}}, \tag{61}$$

where $R_{i,k}^{\max}$ is the maximum rate of the kth user when there are no other users in the system, ie, it is calculated by doing single-user iterative water-filling. As a result, the rate offered by conventional OMA is minimum, but its outage probability is low, which increases the overall outage capacity of the conventional OMA system. The *outage capacity* is defined as the maximum rate that can be maintained by each user multiplied with the success probability of the users. It shows a clear picture of system performance for both data rates and success of each user. The outage capacity analysis of SBD-NOMA is evaluated in Figure 3. The SBD-NOMA system performs well in terms of outage capacity as shown. We can derive an interesting result by combining Figures 2 and 3: that although the conventional UL NOMA achieves maximum sum capacity, it increases the receiver complexity and outage probability to a great extent, which is practically not desired especially if the number of users in a system is large. The same reason lies behind the intersection of curves in Figure 3. As shown in Figure 2, NOMA offers higher data rates, and its sum capacity generally improves with the increase in the number of users. However, by incorporating more users within the same subband, the intraset interference increases. Therefore, NOMA has a high outage probability. Although, the other schemes offer better coverage probability, and hence, their outage probability is quite low, and they offer less complexity than the conventional NOMA technique but their data rates are low. By combining the 2 parameters, the curves intersect in Figure 3. Hence, in situations where the priority is reduced receiver complexity and cost and enhanced QoS, SBD-NOMA schemes should be preferred over conventional UL NOMA, which provide a better rate and a fairly reliable transmission scheme.

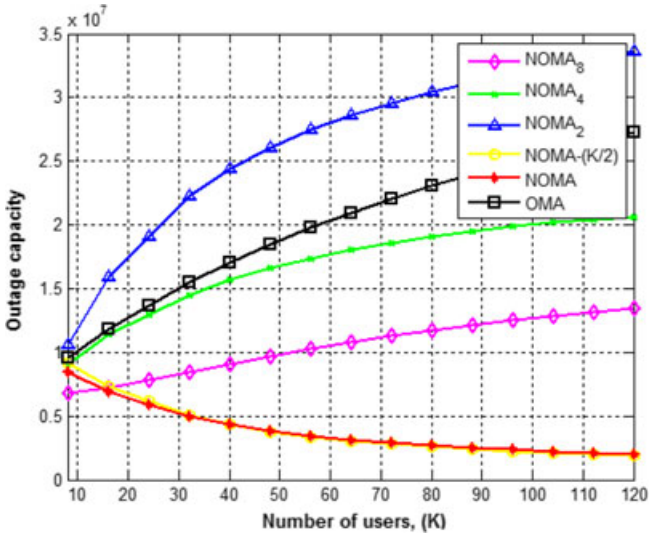

FIGURE 3 Outage capacity of orthogonal multiple access (OMA), nonorthogonal multiple access (NOMA), and the proposed successive bandwidth division scheme

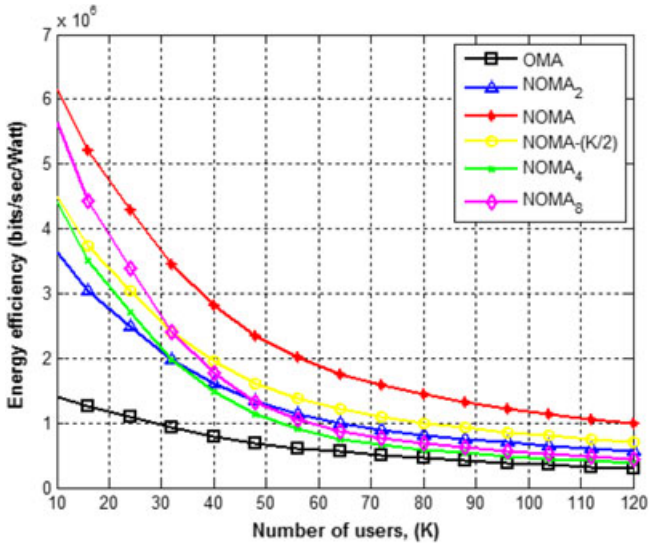

FIGURE 4 Energy efficiency of successive bandwidth division nonorthogonal multiple access (NOMA) with orthogonal multiple access (OMA) and NOMA techniques

Figure 4 reveals the EE of a hybrid SBD-NOMA scheme with increasing number of users. *Energy Efficiency* (η_{EE}), defined in bits per second per watt, is the amount of energy required by the system to transmit data and is expressed as

$$\eta_{\text{EE}} = \frac{R_{\text{sum}}}{P_T} = \frac{\sum_{m=1}^{K/P} \sum_{j=1}^{P/2} W_{\text{sb}} \log_2 \left(1 + \text{SINR}_{i,j}\right)}{P_T}, \tag{62}$$

where P_T is the total transmit power of the system. The trend shows that as the number of users increases, the total transmit power increases; thus, there is an increases in the total sum rate. However, there is a reduction in EE with increasing number of users.

In Figure 5, the impact of cell radius on the performance of OMA, NOMA, and SBD-NOMA is demonstrated. It can be seen that SBD-NOMA performs better than the conventional NOMA if the cell radius is assumed to be very small. However, NOMA outperforms at other values, but as the cell radius increases, the interset interference offered to NOMA by the weak set also enhances, which increases the decoding complexity at the receiver side.

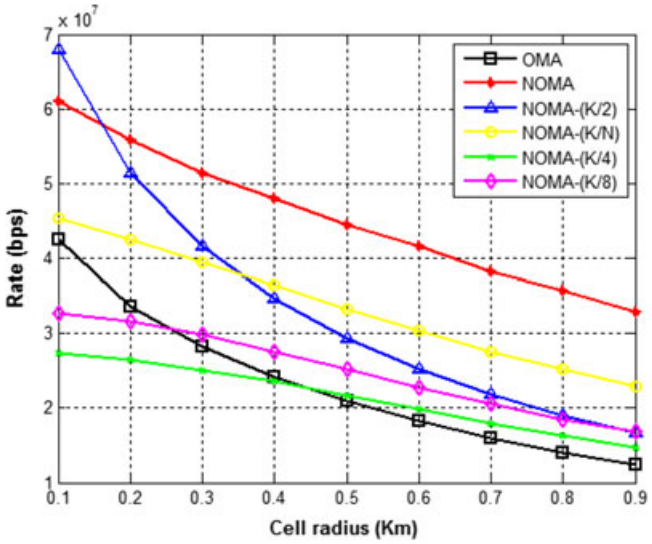

FIGURE 5 Impact of cell radius on the successive bandwidth division scheme ($N = 2$, $K = 40$). NOMA, nonorthogonal multiple access; OMA, orthogonal multiple access

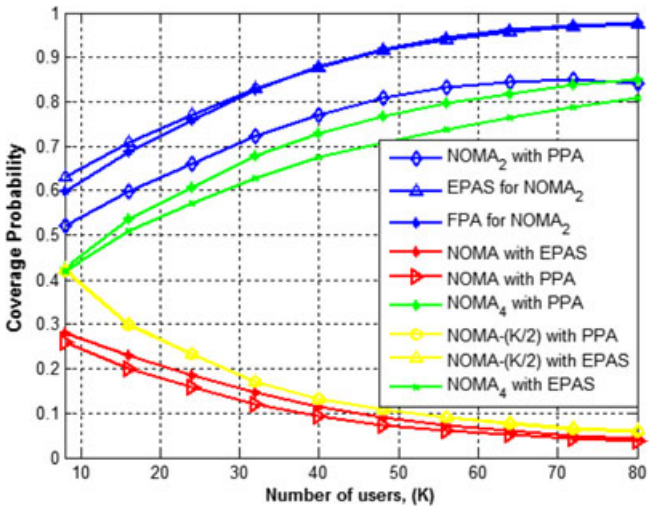

FIGURE 6 Coverage probability comparison of nonorthogonal multiple access $(NOMA)_2$ with different power allocation schemes and NOMA technique. EPAS, equal power allocation scheme; FPA, fixed power allocation; PPA, proposed power allocation.

Figure 6 depicts the coverage probability of conventional NOMA and SBD-NOMA with different power allocation schemes. *Coverage probability* is defined as the probability that a certain number of users achieves a data rate greater than the target data rate. It can be easily seen that SBD-NOMA performs well as compared with NOMA in terms of coverage probability. The coverage probability of FPA and EPAS is even better in this case as compared with the proposed approach; however, EPAS being the simplest criteria of allocating power to users does not perform well, as it allocates equal power to all users and, therefore, treats the weak users in the same manner as the strong ones. The SBD-NOMA system provides every pair a power value that suits their channel gain, which allows a balance between the required power, fairness, and the target rate with the total power allocation constraint across each subband. Although the optimal NOMA scheme shows a greater sum rate, its coverage probability in this scenario is less than the optimal solution. The same trend is depicted in Figure 6.

Figure 7 shows the outage capacity of SBD-NOMA with the conventional NOMA scheme. The outage capacity is larger for SBD-$NOMA_2$ with the proposed power allocation scheme. However, with equal power allocation, the system treats the weak users in the same way as strong users. As strong users get significant interference from weak users, the capacity of strong users gets degraded. The optimal power allocation in SBD-NOMA ensures fairness in the system by imposing an upper limit on each user's individual data rate as compared with the EPAS and FPA schemes. From this Figure, it is clear that the proposed power allocation scheme performs better than the existing ones.

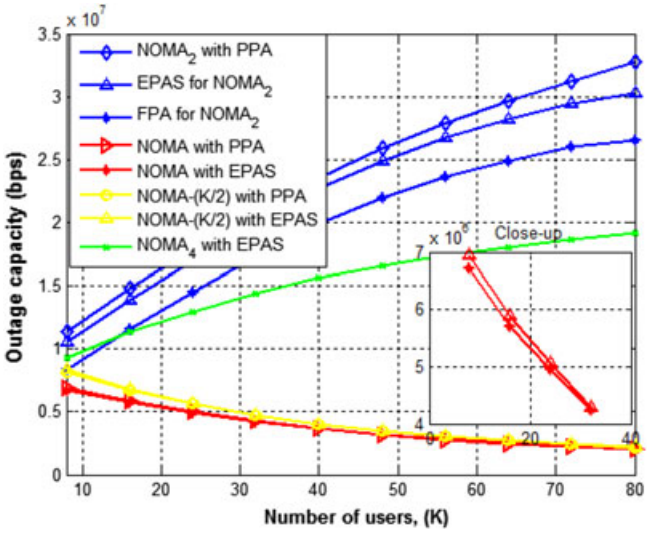

FIGURE 7 Outage capacity comparison of nonorthogonal multiple access $(NOMA)_2$ with different power allocation schemes and the NOMA technique. EPAS, equal power allocation scheme; FPA, fixed power allocation; PPA, proposed power allocation.

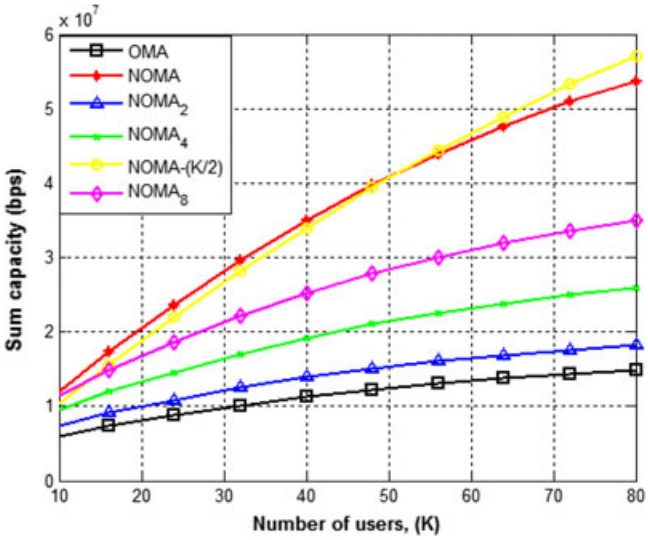

FIGURE 8 Sum capacity comparison of successive bandwidth division nonorthogonal multiple access (NOMA) for $K \geq N$. OMA, orthogonal multiple access

Figures 8 and 9 depict the sum capacity and outage probability of SBD-NOMA with no intraset interference. It can be observed from the Figure that with no intraset interference, the sum rate is inversely proportional to the number of subbands. However, $NOMA_{K/2}$ nominates NOMA with increasing number of users. This is because of the minimum weak-set interference. The outage probability for $K \geq N$ is less as compared with the conventional SBD-NOMA discussed above. The same trend is shown in the Figure.

6 | CONCLUSION

This paper has investigated the performance of SBD-NOMA, which is an OFDMA-based NOMA system with other multiple access schemes, namely, OMA and NOMA. It can be seen that in general, NOMA has more decoding complexity. It introduces some controllable interference at the receiver to realize overloading due to which it can support massive connectivity and higher spectral efficiency. It also requires greater number of SIC for decoding, which requires complex receiver designing. The complexity of SBD-NOMA lies between NOMA and OMA. The depth of SIC in SBD-NOMA is much less than the NOMA system. It also requires a receiver of moderate complexity. The SBD-NOMA sum rate also lies midway between NOMA and OMA. However, it offers minimum error variance because of the reduced depth of SIC and moderate receiver complexity. On

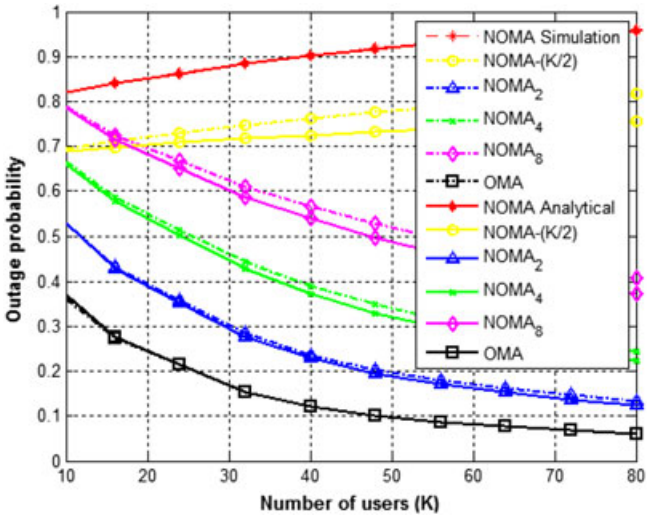

FIGURE 9 Outage probability of successive bandwidth division nonorthogonal multiple access (NOMA) for $K \geq N$. OMA, orthogonal multiple access

the other hand, OMA offers least complexity and is therefore a reasonable choice for achieving good system-level throughput in packet domain services using channel-aware time and frequency domain scheduling. However, OMA cannot provide the further enhancements in quality of experience required at the cell edge user. Furthermore, MIMO NOMA offers larger sum rate capacity as compared with MIMO OMA except when there is a single user. The reason behind the larger sum rate is the power split for which MIMO NOMA achieves larger sum rates. Hence, in a situation where the user requirement is reduced complexity, enhanced rates, better quality of service, and fairly reliable transmission schemes, SBD-NOMA should be prefered. In situations where the user requirement is higher sum rates, NOMA should be preferred as the BS can easily cope with decoding complexity as it has more power. In situations where the user requirement is reduced rates with no interference and simple single-user detection, OMA is prefered. This paper also discussed the approximate closed-form expressions for the outage probability of strong and weak users in SBD-NOMA. The results presented herein paint a favorable picture that SBD-NOMA performs better than NOMA in terms of achievable rates. The proposed SBD scheme also offered better sum rates with reduced complexity especially in massive access scenarios. The proposed scheme under different path loss and power allocation outperformed the EPAS and FPA schemes.

ACKNOWLEDGEMENT

This work was funded, in part, by the Ministry of Education and Science of the Russian Federation Grant No. 02.G25.31.0190 dated 04.27.2016 and performed in accordance with Russian Government Resolution No. 218 of 09.04.2010. The authors also acknowledge the contribution of the COST Action on Inclusive Radio Communications (IRACON) CA15104.

ORCID

Soma Qureshi http://orcid.org/0000-0001-6162-0447
Syed Ali Hassan http://orcid.org/0000-0002-8572-7377

REFERENCES

1. Chih-Lin I, Rowell C, Han S, Xu Z, Li G, Pan Z. Toward green and soft: a 5G perspective. *IEEE Commun Mag*. 2014;52(2):66-73.
2. Thompson J, Ge X-L, Wu H-C, et al. 5G wireless communication systems: Prospects and challenges. *IEEE Commun Mag*. 2014;52(2):62-64.
3. Wang P, Xiao J, Ping L. Comparison of orthogonal and non orthogonal approaches to future wireless cellular systems. *IEEE Veh Technol Mag*. 2006;1(3):4-11.
4. Saito Y, Kishiyama Y, Benjebbour A, Nakamura T, Li A, Higuchi K. Non-orthogonal multiple access (NOMA) for cellular future radio access. Paper presented at: 77th IEEE Vehicular Technology Conference (VTC Spring); 2013.
5. Ding Z, Adachi F, Poor HV. The application of MIMO to non-orthogonal multiple access. *IEEE Trans Wireless Commun*. 2016;15(1):537-552.
6. Ding Z, Yang Z, Fan P, Poor HV. On the performance of non-orthogonal multiple access in 5G systems with randomly deployed users. *IEEE Signal Process Lett*. 2014;21(12):1501-1505.

7. Hojeij MR, Farah J, Nour C, Douillar C. Resource allocation in downlink non-orthogonal multiple access (NOMA) for future radio access. Paper presented at: 81st IEEE Vehicular Technology Conference (VTC Spring); 2015.
8. Choi J. Minimum power multicast beamforming with superposition coding for multiresolution broadcast and application to NOMA systems. *IEEE Trans Commun*. 2015;63(3):791-800.
9. Sun Q, Han S, Chin-Lin I, Pan Z. On the ergodic capacity of MIMO NOMA systems. *IEEE Wireless Commun Lett*. 2015;4(4):405-408.
10. Larsson E, Edfors O, Tufvesson F, Marzetta T. Massive MIMO for next generation wireless systems. *IEEE Commun Mag*. 2014;52(2):186-195.
11. Higuchi K, Kishiyama Y. Non-orthogonal access with random beamforming and intra-beam SIC for cellular MIMO downlink. Paper presented at: IEEE 78th Vehicular Technology Conference (VTC Fall); 2013.
12. Liu Y, Elkashlan M, Ding Z, Karagiannidis GK. Fairness of user clustering in MIMO non-orthogonal multiple access systems. *IEEE Commun Lett*. 2016;20(7):1465-1468.
13. Higuchi K, Kishiyama Y. Non-orthogonal access with random beamforming and intra-beam SIC for cellular MIMO downlink. Paper presented at: Proceedings IEEE Vehicular Technology Conference. (VTC Fall); September 2013.
14. Hanif MF, Ding Z, Ratnarajah T, Karagiannidis GK. A minorization-maximization method for optimizing sum rate in the downlink of non-orthogonal multiple access systems. *IEEE Trans Signal Process*. 2016;64(1):76-88.
15. Choi J. On the power allocation for MIMO-NOMA systems with layered transmissions. *IEEE Trans Wireless Commun*. 2016;15(5):3226-3237.
16. Ding Z, Schober R, Poor HV. On the design of MIMO-NOMA downlink and uplink transmission. Paper presented at: Proceedings IEEE International Conference Communications; June 2016; Kuala Lumpur, Malaysia.
17. Qi S, Han S, Chin-Lin I, Pan Z. On the ergodic capacity of MIMO NOMA systems. *IEEE Wireless Commun Lett*. 2015;4(4):405-408.
18. Dai L, Wang B, Yuan Y, Han S, Chin-Lin I. Non orthogonal multiple access for 5G: solutions, challenges, opportunities, and future research trends. *IEEE Commun Mag*. 2015;53(9):74-81.
19. Liu F, Mähönen P, Petrova M. Proportional fairness-based user pairing and power allocation for non-orthogonal multiple access. Paper presented at: IEEE 26th Annual International Symposium on Personal, Indoor, and Mobile Radio Communications (PIMRC); 2015.
20. Di B, Song L, Li Y. Sub-channel assignment, power allocation, and user scheduling for non-orthogonal multiple access networks. *IEEE Trans Wireless Commun*. 2016;15(11):7686-7698.
21. Kim B, Chung W, Lim S, et al. Uplink NOMA with multi-antenna. Paper presented at: 81st IEEE Vehicular Technology Conference (VTC Spring); 2015.
22. Ding Z, Fan P, Poor V. Impact of user pairing on 5G non-orthogonal multiple access downlink transmissions. *IEEE Trans Veh Technol*. 2016;65(8):6010-6023.
23. Al-Imari M, Xiao P, Imran MA, Tafazolli R. Uplink non-orthogonal multiple access for 5G wireless networks. Paper presented at: 11th International Symposium on Wireless Communication Systems (ISWCS); 2014.
24. Qureshi S, Hassan SA. MIMO uplink NOMA with successive bandwidth division. Paper presented at: IEEE Wireless Communication Networking Conference (WCNC Workshops); 2016.
25. Wang B, Dai L, Zhang Y, Mir T, Li J. Dynamic compressive sensing-based multi-user detection for uplink grant-free NOMA. *IEEE Commun Lett*. 2016;20(11):2320-2323.
26. Chen S, Peng K, Jin H. A suboptimal scheme for uplink NOMA in 5G systems. Paper presented at: IEEE International Wireless Communication and Mobile Computing Conference (IWCMC); 2015.
27. Endo Y, Kishiyama Y, Higuchi K. Uplink non-orthogonal access with MMSE-SIC in the presence of inter-cell interference. Paper presented at: Proceedings IEEE ISWCS; 2012.
28. Sung CW, Fu Y. A game-theoretic analysis of uplink power control for a non-orthogonal multiple access system with two interfering cells. Paper presented at: Proceedings IEEE VTC Spring; 2016.
29. Takeda T, Higuchi K. Enhanced user fairness using non-orthogonal access with SIC in cellular uplink. Paper presented at: Proceedings IEEE VTC; September 2011; Fall.
30. Endo Y, Kishiyama Y, Higuchi K. Uplink non-orthogonal access with MMSE-SIC in the presence of inter-cell interference. Paper presented at: Proceedings IEEE ISWCS; 2012.
31. Sung CW, Fu Y. A game-theoretic analysis of uplink power control for a non-orthogonal multiple access system with two interfering cells. Paper presented at: Proceedings IEEE VTC. Spring; 2016.
32. Shin W, Vaezi M, Lee B, Love DJ, Lee J, Poor HV. Non-orthogonal multiple access in multi-cell networks: Theory, performance, and practical challenges. arXiv:1611.01607; 2016.
33. Fu Y, Salaün L, Sung CW, Chung CS, Coupechoux M. Double iterative waterfilling for sum rate maximization in multicarrier NOMA systems. Paper presented at: IEEE International Conference on Communication (ICC); 2017.
34. Lei L, Yuan D, Ho CK, Sun S. Joint optimization of power and channel allocation with non-orthogonal multiple access for 5G cellular systems. Paper presented at: Proceedings IEEE Global Communication Conference; December 2014.
35. Ding Z, Peng M, Poor HV. Cooperative non-orthogonal multiple access in 5G systems. *IEEE Commun Lett*. 2015;19(8):1462-1465.
36. Naqvi SAR, Hassan SA. Combining NOMA and mmWave technology for cellular communication. Paper presented at: IEEE Vehicular Technology Conference (VTC Fall); September 2016.
37. Saito Y, Benjebbour A, Kishiyama Y, Nakamura T. System-level performance evaluation of downlink non-orthogonal multiple access (NOMA). Paper presented at: PIMRC; 2013.
38. Al-Abbasi ZQ, So DKC. Power allocation for sum rate maximization in non-orthogonal multiple access system. Paper presented at: IEEE 26th Annual International Symposium on Personal, Indoor, and Mobile Radio Communications (PIMRC); 2015.
39. Parida P, Das SS. Power allocation in OFDM based NOMA systems: a DC programming approach. Paper presented at: IEEE Global Telecommunication Conference (GLOBECOM Workshops); 2014.

40. Otao N, Kishiyama Y, Higuchi K. Performance of non-orthogonal multiple access with SIC in cellular downlink using proportional fair-based resource allocation. *IEICE Trans Commun*. 2015;98(2):344-351.
41. Al-Imari M, Xiao P, Ali Imran M. Receiver and resource allocation optimization for uplink NOMA in 5G wireless network. Paper presented at: IEEE International Symposium on Wireless Communication Systems (ISWCS); 2015.
42. Tabassum H, Ali MS, Hossain E, Hossain MJ, Kim DI. Non-orthogonal multiple access (NOMA) in cellular uplink and downlink: Challenges and enabling techniques. arXiv:1608.05783; 2016.
43. Yu W, Rhee W, Boyd S, Cioffi J. Iterative water-filling for Gaussian vector multiple-access channels. *IEEE Trans Inf Theory*. 2004;50(1):145-152.

How to cite this article: Qureshi S, Hassan SA, Jayakody DNK. Divide-and-allocate: An uplink successive bandwidth division NOMA system. *Trans Emerging Tel Tech*. 2017;e3216. https://doi.org/10.1002/ett.3216

APPENDIX

PROOF OF LEMMA 1

The achievable sum rate of the system given by Equation 17 is expanded as

$$R_{\text{sum}} = \frac{1}{\ln 2}\sum_{m} W_{\text{sb}} R_{\text{rr}}, \tag{A1}$$

where

$$R_{\text{rr}} = \ln\left(\sum_{j=1,j\neq n}^{P/2} \varphi_{bjn}\alpha_{2,j} + \sigma_n^2 + \varphi_{bn}\alpha_{2,n}\right) - \ln\left(\sum_{j=1,j\neq n}^{P/2} \varphi_{ajn}\alpha_{1,j} + \sum_{j=1}^{P/2} \varphi_{cjn}\alpha_{2,j} + \sigma_n^2\right) - \ln\left(\sum_{j=1,j\neq n}^{P/2} \varphi_{bjn}\alpha_{2,j} + \sigma_n^2\right) + \ln\left(\varphi_{an}\alpha_{1,n} + \sum_{j=1,j\neq n}^{P/2} \varphi_{ajn}\alpha_{1,j} + \sum_{j=1}^{P/2} \varphi_{an}\alpha_{2,j} + \sigma_n^2\right), \tag{A2}$$

where $\varphi_{an}=|\mathbf{z}_{1,n}\cdot\mathbf{h}_{1,n}|^2$, $\varphi_{bn}=|\mathbf{z}_{2,n}\cdot\mathbf{h}_{2,n}|^2$, $\varphi_{cn}=|\mathbf{z}_{1,n}\cdot\mathbf{h}_{2,n}|^2$, and $\varphi_{cjn}=|\mathbf{z}_{1,n}\cdot\mathbf{h}_{2,j}|^2$, and

$$R_{\text{sum}} = \frac{1}{\ln 2}\sum_{m} W_{\text{sb}}\left[\ln\left(\sum_{j=1,j\neq n}^{P/2} \varphi_{bjn}\alpha_{2,j} + \sigma_n^2 + \varphi_{bn}\alpha_{2,n}\right) + \ln\left(\varphi_{an}\alpha_{1,n} + \sum_{j=1,j\neq n}^{P/2} \varphi_{ajn}\alpha_{1,j} + \sum_{j=1}^{P/2} \varphi_{cjn}\alpha_{2,j} + \sigma_n^2\right) - \ln\left(\sum_{j=1,j\neq n}^{P/2} \varphi_{ajn}\alpha_{1,j} + \sum_{j=1}^{P/2} \varphi_{cjn}\alpha_{2,j} + \sigma_n^2\right) - \ln\left(\sum_{j=1,j\neq n}^{P/2} \varphi_{bjn}\alpha_{2,j} + \sigma_n^2\right)\right]. \tag{A3}$$

To prove Lemma 1, we need to find the Hessian matrix of Equation A2. For this, take the second derivative with respect to $\alpha_{1,n}$ and $\alpha_{2,n}$.

$$\partial R_{\text{rr}}/\partial\alpha_{1,n}^2 = \frac{-\varphi_{an}^2}{\left(\varphi_{an}\alpha_{1,n} + \sum_{j=1,j\neq n}^{P/2} \varphi_{ajn}\alpha_{1,j} + \sum_{j=1}^{P/2} \varphi_{cjn}\alpha_{2,j} + \sigma_n^2\right)^2} \tag{A4}$$

$$\partial R_{\text{rr}}/\partial\alpha_{2,n}^2 = \frac{-\varphi_{cn}^2}{\left(\varphi_{an}\alpha_{1,n} + \sum_{j=1,j\neq n}^{P/2} \varphi_{ajn}\alpha_{1,j} + \sum_{j=1}^{P/2} \varphi_{cjn}\alpha_{2,j} + \sigma_n^2\right)^2} + \frac{\varphi_{cn}^2}{\left(\sum_{j=1,j\neq n}^{P/2} \varphi_{ajn}\alpha_{1,j} + \sum_{j=1}^{P/2} \varphi_{cjn}\alpha_{2,j} + \sigma_n^2\right)^2} - \frac{\varphi_{bn}^2}{\left(\sum_{j=1,j\neq n}^{P/2} \varphi_{bjn}\alpha_{2,j} + \sigma_n^2 + \varphi_{bn}\alpha_{2,n}\right)^2} \tag{A5}$$

$$\partial R_{\text{rr}}/\partial\alpha_{1,n}\partial\alpha_{2,n} = \frac{-\varphi_{an}\varphi_{cn}}{\left(\varphi_{an}\alpha_{1,n} + \sum_{j=1,j\neq n}^{P/2} \varphi_{ajn}\alpha_{1,j} + \sum_{j=1}^{P/2} \varphi_{cjn}\alpha_{2,j} + \sigma_n^2\right)^2} \tag{A6}$$

As the Hessian matrix is negative semidefinite, because for any vector, the answer will always be ≤ 0, which implies that it is concave in nature. This has been proved by following the arguments similar to the one made in the work of Choi.[15]